Novel insights into mannitol metabolism in the fungal plant pathogen Botrytis cinerea

Thierry Dulermo, Christine Rascle, Geneviève Billon-Grand, Elisabeth Gout, Richard Bligny, Pascale Cotton

NOVEL INSIGHTS INTO MANNITOL METABOLISM IN THE FUNGAL PLANT PATHOGEN *BOTRYTIS CINEREA*

Authors : Thierry Dulermo[*†], Christine Rascle[*], Geneviève Billon-Grand[*], Elisabeth Gout[‡], Richard Bligny[‡] and Pascale Cotton[§]

Address
*Génomique Fonctionnelle des Champignons Pathogènes des Plantes, UMR 5240 Microbiologie, Adaptation et Pathogénie, Université de Lyon, Lyon, F-69003, France ; Université Lyon1- CNRS-INSA-BayerCropScience, 10 rue Pierre Baizet, F-69009, Lyon, France, †Laboratoire de Microbiologie et Génétique Moléculaire, CNRS UMR 2585, INRA UMR1238, AgroParisTech, INRA, centre de Versailles-Grignon BP 01, F-78850 Thiverval-Grignon, France, ‡Physiologie Cellulaire et Végétale, UMR 5168, Institut de Recherche en Technologies et Sciences pour le Vivant, CEA, 17 rue des Martyrs, 38054 Grenoble cedex 9, France, §Génétique Moléculaire des Levures, UMR 5240 Microbiologie, Adaptation et Pathogénie, Université de Lyon, Lyon, F-69003, France ; Université Lyon1- CNRS-INSA-Bayer CropScience, 10 rue Raphaël Dubois, Bât Lwoff, Villeurbanne, F-69621, France

For correspondence. E-mail pascale.cotton@univ-lyon1.fr; Tel +33472448030; Fax +33 472432686
Short title : Mannitol pathway in *Botrytis cinerea*

SYNOPSIS

In order to redefine the mannitol pathway in the necrotrophic plant pathogen *Botrytis cinerea*, we used a targeted deletion strategy of genes encoding two proteins of mannitol metabolism, a mannitol dehydrogenase (BcMTDH), and a mannitol-1-phosphate dehydrogenase (BcMPD). Mobilization of mannitol and quantification of *Bcmpd* and *Bcmtdh* gene transcripts during development and osmotic stress confirmed a role for mannitol as temporary and disposable carbon storage compound. In order to study metabolic fluxes, we followed conversion of labelled hexoses by wild type and *Bcmpd* and *Bcmtdh* mutant strains by *in vivo* NMR spectroscopy. Our data revealed that glucose and fructose were metabolized via the BcMPD and BcMTDH pathways, respectively. Existence of a novel mannitol phosphorylation pathway was suggested by NMR investigations. This last finding definitively challenged the existence of the originally postulated mannitol cycle in favor of two simultaneously expressed pathways. Finally, physiological and biochemical studies conducted on double deletion mutants (*Bcmpd*/*Bcmtdh*) showed that mannitol was still produced despite a complete alteration of both mannitol biosynthesis pathways. This strongly suggests that one or several additional undescribed pathways could participate to mannitol metabolism in *B. cinerea*.

Key words:
Botrytis cinerea, *in vivo* NMR spectroscopy, mannitol, carbon metabolism, osmotic stress, trehalose.
Abbreviations used: BcMPD, *Botrytis cinerea* MPD; BcMTDH, *Botrytis cinerea* MTDH; MPD, mannitol-1-phosphate dehydrogenase; MTDH, mannitol dehydrogenase; PCA, perchloric acid; TLC, thin layer chromatography.

INTRODUCTION

Mannitol is one of the most abundant polyols occurring in nature. It is usually the most abundant soluble carbohydrate within the mycelium [1]. In fungi, several physiological functions have been ascribed to D-mannitol, such as reservoir of reducing power [2], carbon storage compound accumulated in *Agaricus bisporus* basidiospores [3] or necessary for the formation of fruit bodies in *Stagonospora nodorum* [4]. Mannitol contributes to stress tolerance in fungi. In *Aspergillus niger*, mannitol appears to be essential for the protection of spores against cell damage under a variety of stress conditions including cold, drought and oxidative stress [5]. In mycorrhizal fungi, mannitol plays the role of carbon translocation compound that enables fungi to assimilate carbohydrates from plant origin [6, 7]. Furthermore, mannitol has a role in fungal-plant interactions. During the biotrophic interaction *Uromyces fabae*/*Vicia faba*, levels of mannitol markedly increase in apoplastic fluids of infected leaves and in spores. Mannitol might have a dual function, sequestration of plant hexoses and protection against reactive oxygen species [8]. A role for mannitol in pathogenicity of *Alternaria alternata* on its host, tobacco, was demonstrated [9, 10]. Mannitol was secreted by *A. alternata* in response to tobacco extracts. In addition, tobacco expressed an endogenous mannitol dehydrogenase during infection [9, 11]. Mannitol, secreted by *A. alternata* could play an antioxidant role and quench reactive oxygen species. Mannitol dehydrogenase, induced in plant by fungal colonization, degrades pathogen-produced mannitol, allowing for ROS-mediated plant defense to be effective against the fungus.

The metabolic pathway for mannitol biosynthesis and catabolism (Figure. 1), well described in filamentous fungi, takes place through the mannitol cycle, involving two pathways [12]. The direct reduction of fructose-6-phosphate into mannitol-1-phosphate involves a mannitol-1-phosphate dehydrogenase (MPD, EC 1.1.1.17). Mannitol-1-phosphate is then dephosphorylated into mannitol via a mannitol-1-phosphate phosphatase. This last reaction was described as irreversible, consequently, mannitol degradation is supposed to occur through oxidation of mannitol to fructose via a reversible mannitol dehydrogenase (MTDH, EC 1.1.1.138). Both pathways exist in ascomycetes [2].

However, recent reports have challenged the existence of a mannitol cycle. In *S. nodorum*, MPD is necessary for mannitol catabolism, whereas MTDH is not [4, 13]. A mannitol phosphorylation pathway allowing conversion of mannitol into mannitol-1-phosphate might exist. Mannitol pathway explorations conducted in *S. nodorum* and *A. alternata* revealed that mannitol synthesis occurred mainly through MPD [13, 14]. *mpd* deletion mutant strains revealed an intracellular mannitol concentration decreased by more than 80%, whereas *mtdh* strains were almost completely phenotypically wild type. While mannitol metabolism through mannitol-1-phosphate appears to be the dominant route, the physiological role of MTDH branch remains unclear.

In a previous report, we showed that mannitol was accumulated during infection of sunflower by the necrotrophic plant pathogen *B. cinerea* [15]. During pathogenesis, plant hexoses were converted into mannitol, which was the major soluble carbon compound detected in infected tissues. In previous experiments, we were unable to detect mannitol in fungal growth media [15]. This polyol could be used as translocation compound to sequester plant hexoses. Moreover, mannitol accumulated mainly during the final steps of fungal development *in planta*, being stored when conidiophores emerged. Mannitol could be necessary for spore survival or constitute a source of energy for germination. By means of reverse genetics and metabolic investigations, we have explored the physiological role and functioning of the mannitol pathway in *B. cinerea*.

EXPERIMENTAL

Fungal strain and growth conditions

Botrytis cinerea B05.10 was maintained at 21°C on rich medium as described in [16]. *B. cinerea* developmental stages were obtained from mycelia grown for 2 or 6 days (mycelium and sporulating mycelium) on cellophane sheets deposited on 2% glucose-rich solid medium. Conidia were harvested from 12-day-old mycelium grown on 2% glucose-rich solid medium. Germinating conidia were obtained by cultivating 12-days-old spores (10^7 ml^{-1}) in 2% glucose-rich liquid medium (110 rpm). For osmotic stress experiments, mycelia were grown for 2 days on cellophane on solid Gamborg medium (pH 5.0) supplemented with 2% glucose [16]. Mycelia were then transferred for 30 min, 1 h, 4 h, 9 h, and 24 h on fresh solid medium supplemented with 2% glucose and 1M NaCl. For osmotic stress response analysis by *in vitro* NMR spectroscopy, mycelia were first transferred for 4 h on labelled fructose plates (1% fructose containing 10% ^{13}C-fructose) and transferred for 1 and 4 h on fresh solid medium supplemented with 2% glucose and 1M NaCl. Mycelia, conidia and germinating conidia were harvested, frozen in liquid nitrogen then stored at -80°C. *In vivo* NMR analyses were performed in a perfusion medium containing 1 g l^{-1} KNO_3, 0.05 g l^{-1} KCl, 0.1 g l^{-1} $MgSO_4$, 0.1 g l^{-1} $CaSO_4$, and ^{13}C-labelled glucose or fructose as indicated in text. *B. cinerea* transformant strains were selected on rich media supplemented with 70 µg ml^{-1} hygromycin (Invivogen, Toulouse, France) or with 100 µg ml^{-1} nourseothricin (Werner BioAgents, Jena, Germany).

***In vitro* germination and conidiation assays**

Conidia were harvested in 0.5% Tween 80 from 12-days-old mycelium grown on solid rich medium. For *in vitro* germination assays, 500 conidia of each strain were spread on solid rich medium in 140 mm plates. Young germinations were counted after 4 days of incubation. For conidiation assays, 1000 conidia were spread on solid rich medium in 24-well-plates. After 12 days of growth, conidia produced in each well were harvested and counted.

Pathogenicity tests

Phytopathogenicity assays were performed on sunflower cotyledons as hosts as previously described [15]. Cotyledons from 1-week-old germlings were infected at the end of a dark period by depositing a 5-mm-mycelium disk near the tip of the leaves. Necrosis was detectable 24 hpi (hours post infection) by the appearance of a brown color surrounding the starting point of infection. At 48 hpi, half of the cotyledons were macerated and necrosed. The whole cotyledon was infected at 72 hpi. Conidiation began at 96 hpi and was achieved at 120 hpi.

Plasmid construction and transformation of *B. cinerea*

Transformation of *B. cinerea* B05.10 was performed using the *hph* gene as selectable marker. To disrupt *Bcmpd* and *Bcmtdh,* constructs containing the hygromycin resistance cassette (*OliC* promoter-*hph* gene coding sequence- *tub1*terminator) flanked by 5' and 3'*Bcmpd* and *Bcmtdh* genomic DNA fragments were realized (Figure S1). The hygromycin cassette was released from pLOB1 (provided by P. Tudzynski, Münster, Germany) after *EcoR*I and *EcoR*V digestion, and then cloned in pBKSII. Flanking regions (*5'Bcmpd, 3'Bcmpd*, *5'Bcmtdh* and *3'Bcmtdh* fragments) amplified using P1/P2, P3/P4, P5/P6 and P7/P8 primers respectively (Table S1 and Figure S1) were cloned on every side of the hygromycin cassette (Figure S1) to form pTD5 and pTD6. To obtain pTD10 plasmid, *Bcmtdh* 5' and 3' flanking regions were

amplified using P9/P10 and P11/P12 respectively (Figure S1). Amplified fragments were cloned in pCB04, on each side of the nourseothricin cassette, which contained the S*treptomyces* nourseothricin N-acetyl-transferase gene (*nat1*) flanked by the *A. nidulans OliC* promoter and the *B. cinerea tub1* terminator [17]. Preparation of protoplasts and transformation were adapted from procedures described in [18]. Fungal cell wall was digested using 50 mg ml^{-1} Glucanex (Novozymes, Dittengen, Switzerland) for 2 h at 26°C. Wild type strain (WT) was transformed with 10 µg of *Not*I linearized vector pTD5 or pTD6 to obtain *Bcmtdh* and *Bcmpd* mutants respectively. The development of a double mutant was achieved by transforming the previously generated *ΔBcmpd* strain with 10 µg of *Sca*I linearized vector pTD10. PCR analyses were performed to ensure replacement of gene of interest by the selection cassette. gDNA from *Bcmpd* transformants was amplified using P13/P14 and P15/P16 primers (Table S1), to check 5' and 3' insertions respectively. gDNA from *Bcmtdh* transformants was amplified using P17/P14 primers and P18/P19 primers to verify 5' and 3' insertions respectively (Table S1). *Bcmtdh* gene replacement by the nourseothricin cassette was verified using primers P20/P21 and P22/P19 to check 5' and 3' insertions respectively (Table S1). Southern analyses were performed to ensure single insertions. DNA (5 µg) was digested with *Eco*RI for single mutants, and with *Hind*III for double mutants, separated through an agarose gel (0.8%) and transferred to a nylon membrane. A ^{32}P-labelled probe, (*hph* coding sequence for single mutants or the *5'Bcmtdh* flanking region for double mutants), was obtained from plasmids pLOB1 and pTD5 using Megaprime DNA Labelling system (Amersham Biosciences). Hybridization was carried out as described in [19].

RNA isolation and transcript quantification

Biological materials were frozen in liquid nitrogen and kept at -80°C. Samples were crushed in liquid nitrogen, and total RNAs were extracted by phenol/chloroform separation and lithium chloride precipitation [20]. For Q-PCR experiments, 20 µg of total RNA of each sample were treated with DNAseI (Ambion). Absence of genomic DNA was controlled by PCR using the DNaseI-treated total RNA as template and Taq-DNA polymerase (MP Biomedicals, Solon, USA). Quality of total RNA was verified using Agilent 2100 Bioanalyzer, Agilent RNA 6000 Nano reagents and RNA Chips. Total DNaseI-treated RNA (5 µg) was treated with Thermoscript RT (Invitrogen, Carlsbad, USA) as described by manufacturer. Q-PCR experiments were performed in ABI PRISM 7900HT (Applied Biosystems, Foster City, USA) using the Power SYBR® Green PCR Master Mix (Applied Biosystems) according to the instructions of the manufacturer. Relative quantification was based on the $2^{\Delta CT}$ method using *Bcact1* and *BctubA* as calibrator references. As gene expression profiles were similar using both controls, only the results obtained using *BcactA* transcripts are presented here. The amplification reaction was as follows: 95°C 10 min, 95°C 15 s, and 60°C 1 min (50 cycles), 95°C 15 s, 60°C 15 s, and 95°C 15 s. Three independent replicates, prepared from independent biological samples, were analyzed. Primers used for Q-PCR are shown in Table S1.

NMR spectroscopy

PCA (perchloric acid) extracts were prepared from 5 to 10 g *B. cinerea* mycelia according to the method described in [21]. Values are given in mg g^{-1} fresh weight (FW) of fungal material. *In vitro* (tissue extracts) and *in vivo* (perfused tissues) spectra were recorded on a Bruker NMR spectrometer (AMX 400, wide bore; Bruker, Billerica, MA) equipped either with a 10-mm or a 25-mm multinuclear-probe tuned at 161.9 or 100.6 MHz for ^{31}P- and ^{13}C-analyses. The deuterium resonance of $^{2}H_2O$ was used as lock signal. For *in vitro*

measurements, ^{13}C-NMR and ^{31}P-NMR acquisitions were performed as described in [15]. Assignments and quantifications were made after running a series of spectra of extracts, added with known amounts of authentic compounds, and at differents pHs for the extracts submitted to ^{31}P-NMR analysis, in particular to be certain that the peak of resonance appearing at 4.77 ppm in samples incubated with mannitol corresponded well to mannitol-1-phosphate. *In vivo* measurements were performed using 48 hpi sunflower cotyledons as described in [15].

Polyol and sugar detection by thin layer chromatography (TLC)

Mannitol was extracted from conidia, germinating conidia, mycelia or conidiating mycelia frozen in liquid nitrogen, crushed and then lyophilized. In order to obtain comparable data, 100 mg of dessicated fungal extracts were suspended in 900 µl of water and boiled for 10 min for each sample. Supernatants were analyzed by thin layer chromatography (TLC). One µl of each sample was deposited on TLC-plates SIL G-25 (Macherey-Nagel, France) and separated in acetonitril:ethylacetate:propanol:water (85:20:20:15, by vol). Sugars and polyols were revealed using 0,5% $KMnO_4$, 1N NaOH and identified by using standard sugars or polyols (1 µl of 0.5% standard solution).

Preparation of cell extracts and enzyme assays

Cell extracts were prepared as described in [5]. Lyophilized mycelia were ground, resuspended in extraction buffer (50 mM phosphate buffer pH 7.0, 0.5 mM EDTA, 5mM ß-mercaptoethanol), then centrifuged for 30 min at 15000 rpm at 4°C. Supernatants were collected and desalted on a Zeba Desalt Spin column (ThermoScientific, Cergy Pontoise, France) before enzyme activity measurements. Enzyme assays were performed as described in [22] using 50 µg of proteins in a final volume of 1 ml and by monitoring absorbance changes of NAD(P)+/NAD(P)H at 340 nm. For MTDH activity, the reduction of fructose to mannitol was assayed in a reaction mixture containing 0.6 M fructose, 0.2 mM NADPH, 10 mM HEPES pH 7.0. The oxidation of mannitol to fructose was conducted using 0.4 M mannitol, 2mM NADP, 10 mM HEPES pH 9.0. For MPD activity, the reduction of fructose-6-phosphate was assayed in a reaction mixture containing 5 mM fructose-6-phosphate, 0.3 mM NADH, 10 mM Hepes pH 7.0. For the reverse reaction, the oxidation of mannitol-1-phosphate was measured using 5 mM mannitol-1-phosphate, 0.5 mM NAD, 10 mM HEPES pH 9.0. Enzyme activity was expressed as nmoles of cofactor (NAD(P)H reduced or oxidized) per minute and per µg of total cell extract protein.

Western Blot analysis

BcMPD and BcMTDH were produced as His-tag fusion proteins in *E.coli* M15 using the QiaExpress System (Qiagen, Courtaboeuf, France). cDNAs were amplified by PCR with forward primers containing *Nco*I restriction sites and reverse primers containing *Bgl*II sites (Table S1). PCR products were cloned in pQE60. Optimal protein expression was achieved using 2 mM IPTG after 4 h of induction at 37°C and 1 mM IPTG after 20 h of induction at 23°C, for BcMPD and BcMTDH respectively. BcMPD was detected in inclusion bodies while BcMTDH remained in soluble fraction. Purification of tagged proteins was performed on Ni-NTA columns, under denaturing and native conditions for BcMPD and BcMTDH respectively, according to manufacturer's instructions. Anti-BcMPD and anti-MTDH sera were obtained by immunization of rabbits with the purified proteins (Covalab, Villeurbanne, France). Detection of BcMPD and BcMTDH in fungal strains was performed by Western blot

analyses. Total cell extract proteins were quantified in order to load 75 µg of each extract in each lane. Proteins were then separated by SDS-PAGE in a 10 % acrylamide gel and blotted onto a nitrocellulose membrane. Nitrocellulose membranes were probed with rabbit polyclonal BcMPD (1:2500) and BcMTDH (1:2500) antisera. Bands were visualized with ECL (ElectroChemiLuminescence) using HRP (horseradish peroxidase) conjugated with goat anti-rabbit IgG (dilution 1:40000). The detection was performed as described in the manufacturer's instructions for the ECL Western detection kit (Super Signal West Pico Chemiluminescent Substrate, Perbio, France).

RESULTS AND DISCUSSION

Construction of *Bcmpd* and *Bcmtdh* mutant strains

To understand the role of mannitol in *B. cinerea* (Figure 1), we searched for mannitol dehydrogenase and mannitol-1-phosphate dehydrogenase coding sequences, in order to construct single and double deletion mutant strains. *Bcmtdh* and *Bcmpd* genes were identified in the genome sequence of *B. cinerea* (http://www.broad.mit.edu/annotation/genome/botrytis_cinerea/). Low stringency Southern blot indicated that only one copy of each gene was present in the *B. cinerea* genome (data not shown). Each sequence (respectively 1314 bp and 862 bp for *Bcmpd* and *Bcmtdh*) had one intron. Sequence analyses revealed that BcMPD and BcMTDH had the features of mannitol-1-phosphate 5-dehydrogenases and mannitol 2-dehydrogenases and coded respectively 43 and 28 kDa isoforms. BcMDTH shares 71% and 78% identity with *S. nodorum* Mdh1 and *A. alternata* MtDH, respectively. BcMPD shares 62% and 59% identity with *S. nodorum* Mpd1 and *A. alternata* MpDH, respectively. Whereas BcMPD belongs to the long-chain dehydrogenases/reductases superfamily (LDR), BcMTDH falls into the short-chain group of dehydrogenase/reductase superfamily [23-24].

In the *Bcmpd* deletion construct, a region including 567 bp of the promoter, the open reading frame (ORF) and 328 bp of the 3' of the gene was replaced by a hygromycin resistance cassette. In the case of the *Bcmtdh* deletion vector, 60 bp of the promoter and 423 bp of the coding sequence were replaced by the hygromycin resistance cassette (Figure S1A, B). Protoplasts of *B. cinerea* B05.10 strain were transformed with the linearized vectors and hygromycin-resistant transformants were tested by PCR and Southern analyses (data not shown, Figure S1D). In both cases, two transformants, *ΔBcmpd19* and *ΔBcmpd24,* for *Bcmpd,* and *ΔBcmtdh11* and *ΔBcmtdh16,* for *Bcmtdh*, were found to have undergone gene replacement as expected (Figure S1D). Gene deletions were further confirmed through transcriptional analyses and western blot that revealed an absence of transcripts and proteins in the mutants as compared to the wild type strain (Figure 2A, B). Interestingly, as compared to the wild type strain, *Bcmtdh* expression was clearly increased in *Bcmpd* mutant, whereas *Bcmpd* transcription level was not affected by *Bcmtdh* deletion. Western blot experiments showed that BcMPD and BcMTDH proteins seemed to be more abundant in both deletion mutants (Figure 2B). Enzymatic assays (Figure 2C) confirmed that *Bcmpd* deletion abolished mannitol-1-phosphate dehydrogenase activity. However, in the *Bcmtdh* mutant, mannitol dehydrogenase activity was strongly reduced but not completely eliminated (Figure 2C). Indeed, a low mannitol dehydrogenase activity remained in *Bcmtdh* mutant. All experiments presented in this work were conducted on *Bcmpd19* and *Bcmpd24* for BcMPD pathway and

on *Bcmtdh11* and *Bcmtdh16* for BcMTDH. In both cases, results were clearly similar, in all experiments, for the two mutants analyzed. Consequently, in order to improve reading of the manuscript, results presented here concern *Bcmpd19*, *Bcmtdh16* deletion mutant strains, only.

Conversion of hexoses by BcMPD and BcMTDH pathways

To investigate the respective role of BcMPD and BcMTDH branches in mannitol metabolism, hexose assimilation and conversion through the mannitol pathway were performed in a plant infection context, by *in vivo* NMR spectroscopy. Transfer rates of $^{13}C_1$-glucose or $^{13}C_2$-fructose by *ΔBcmpd* or *ΔBcmtdh* strains were followed in real time using sunflower cotyledons infected by *B. cinerea* (Table 1) and compared to the data previously obtained with the wild type strain [15]. $^{13}C_1$-glucose was converted by *ΔBcmpd* and *ΔBcmtdh* mutant strains into $^{13}C_1$-trehalose, glycogen and $^{13}C_{1/6}$-mannitol as previously shown [15]. Whereas transfer of $^{13}C_1$ from glucose to mannitol was strongly impaired in *ΔBcmpd*, amounts of labelled trehalose and glycogen were increased. In *ΔBcmtdh,* labelling transfer rate of $^{13}C_1$ from glucose into $^{13}C_{1/6}$ mannitol was similar to the WT (wild type) strain, while the amounts of labelled trehalose and glycogen were seriously lowered. $^{13}C_2$-fructose was converted by all the strains in a unique compound, mannitol. However, *ΔBcmtdh* transferred $^{13}C_2$ from fructose to mannitol with a lower efficiency, as compared to the WT strain (30% decrease). *In vivo* NMR data showed trehalose (and glycogen) labelling during growth in the presence of glucose but not in the presence of fructose. Our data clearly demonstrate that trehalose accumulation is a consequence of MPD pathway deletion, preferentially used during glucose assimilation by *B. cinerea.* Trehalose (and glycogen) synthesis is directly linked to glucose-6-phosphate (Figure 1). Mannitol biosynthesis is also connected to this metabolite via fructose-6-phosphate, used as substrate by BcMPD. Consequently, mannitol synthesis from glucose by BcMPD pathway could deplete the pool of glucose-6-phosphate. *Bcmpd* mutants, affected in mannitol biosynthesis, could produce trehalose and glycogen to prevent glucose-6-phosphate accumulation.

Mannitol is mobilized during *in vitro* development of *B. cinerea*

Metabolic profiling revealed that mannitol is found in large amounts in developing *B. cinerea* mycelium [15]. To try to determine the role of mannitol in *B. cinerea* development, we analyzed sporulation and germination rate. No obvious differences were observed between the WT and single mutant strains (Figure S2). This lack of effect of mannitol gene deletion on sporulation and/or spore germination, prompted us to analyze sugar and polyol content by TLC (thin layer chromatography), after growth in the presence of glucose (Figure 3). For this purpose, fungal extracts were analyzed during distinctive phases of development: growing mycelium (2-day-old cultures), conidiation (6-day-old cultures), mature conidia (collected from 12-day-old cultures) and germination of conidia (performed for 2, 4 and 6 hours).

Mannitol, and to a lesser extent trehalose, were accumulated during sporulation and in mature conidia in WT strain. These compounds, rapidly degraded during germination, were almost undetectable 2 hours after germination initiation (Figure 3A). While *ΔBcmtdh* exhibited a similar profile to WT, sugar profile revealed by TLC was modified in *ΔBcmpd*. Mannitol content was markedly reduced in mycelium, whereas trehalose store drastically increased in mature conidia and mycelium (2-d and 6-d old). Surprisingly, TLC profiles revealed an almost unaltered mannitol content in mutant strain conidia.

Bcmpd and *Bcmtdh* gene expression was also checked during development phases, in the WT strain. The results presented in Figure 3B show that both genes exhibited similar

expression patterns during *in vitro* development of WT strain. Despite the dissimilar expression levels, their transcription was particularly high during spore genesis (6-day-old cultures) and in mature conidia. In contrast, during germination, transcript and protein levels drastically decreased (Figure 3B, C). It should be noticed that BcMTDH detection was higher, particularly two hours after germination initiation. This could be explained by a major role played by this protein in mannitol degradation during germination. Nevertheless, both mannitol metabolism branches could participate in mannitol accumulation in conidiating mycelium and spores.

Given its high abundance in spores, the idea of mannitol acting as carbohydrate reserve, as suggested in several reports, can be considered [25, 26]. Data on sporulation and germination rate in fungal pathogens affected in mannitol metabolism by gene disruption strategies are controversial. In *S. nodorum, mpd* and *mpd*/*mtdh* mutants, the production of conidia was strongly affected [4, 13], whereas in *A. alternata, mpd/mtdh* mutant is affected only[10]. As *S. nodorum* and *A. alternata*, *B. cinerea* accumulates mannitol in sporulating mycelium [4, 10] but, despite a lower mannitol content, mutants were not affected for *in vitro* or *in planta* conidiation (Figure S2). A reduced mannitol concentration could allow sporulation. Moreover, trehalose could be stored or degraded instead of mannitol.

Mannitol is involved in osmotic stress response in *B. cinerea*

To further dissect the mannitol pathway, it was necessary to identify physiological conditions that could induce synthesis or degradation of this compound in *B. cinerea*. An osmotic shock is known to induce remobilization of intracellular carbon pool in fungi [27]. Most reports have so far excluded a role for mannitol in enabling fungi to cope with osmotic stress. *Sclerotinia sclerotiorum, Saccharomyces cerevisiae* and *A. nidulans* store glycerol in response to a hyperosmotic stress [28, 29, 30], whereas *Magnaporthe grisea, Cladosporium fulvum* and *S. nodorum* accumulate arabitol [31, 32, 33]. In *B. cinerea,* osmotic stress response is controlled through glycerol accumulation [34]. But mannitol, directly connected to central carbon metabolism could also be implicated in osmotic stress response. To address this question, we investigated the polyol content of *B. cinerea* WT, *Bcmpd* and *Bcmtdh* mutant strains during growth under hyperosmotic conditions (Figure 4A).

In WT strain, mannitol was transiently degraded during stress response. Its concentration decreased between 1 and 4 h of stress and then increased from 9 to 24 h after transfer. In parallel, glycerol accumulated as mannitol was degraded (Figure 4A). Mannitol degradation during osmotic stress response could suggest its contribution to osmo-adaptation. Analysis of *Bcmpd* and *Bcmtdh* gene expression by Q-PCR, revealed that *Bcmpd* was transiently downregulated, whereas *Bcmtdh* transcription increased as mannitol pool decreased (Figure 4B). After one hour of stress, *Bcmtdh* gene expression reached its maximal level. A 4.5 fold expression increase was detected. BcMPD and BcMTDH protein profiles were analyzed by Western blot (Figure 4A). During osmotic stress, BcMPD was degraded from 0 to 1 h whereas BcMTDH was accumulated. Hence, BcMTDH could be preferentially dedicated to mannitol degradation during osmotic stress response.

In *ΔBcmtdh* mutant, TLC profile was similar to that of the WT strain (Figure 4A). *ΔBcmpd* showed a constant and low mannitol content, whereas trehalose, produced by this mutant strain was degraded concomitantly to glycerol accumulation. While in the WT and in the *Bcmtdh* mutant, mannitol pool was partially restored from 9 to 24 h of stress, trehalose pool was not restored in *ΔBcmpd* mutant. Expression profiles of *Bcmpd* or *Bcmtdh* genes in WT and both mutant strains were similar (Figure 4B). However, western blot experiments showed that, in *ΔBcmtdh* strain, BcMPD was not degraded during osmotic stress (from 0 to 4 h). Therefore, while transcriptional control of *Bcmpd* gene was the same, post-translational

control differed in WT and *ΔBcmtdh* mutant. Mannitol content decreased during osmotic stress response in *ΔBcmtdh*. This could be due to the low MTDH activity still detected in *ΔBcmtdh* cell extracts. On the other hand, BcMPD could participate in mannitol degradation. Consequently, this could suggest, contrary to the proposed cycle [12], that the mannitol-1-phosphate dephosphorylation reaction could be reversible to allow mannitol degradation through MPD pathway (Figure 1).

Our data showed that mannitol degradation in WT and *Bcmtdh* strains paralleled glycerol accumulation during osmotic stress response, suggesting that mannitol could constitute a carbon store in which *B. cinerea* could draw, in order to quickly synthesize glycerol for osmoprotection. For this purpose, mannitol pool of *B. cinerea* wild type strain was labelled using $^{13}C_2$-fructose (fructose is almost solely converted in mannitol in WT strain). An osmotic shock (1 M NaCl), in the presence of unlabelled glucose, was applied to mycelium and allocation of labelled carbon during osmotic response was then followed by *in vitro* NMR spectroscopy (Figure S3). Before osmotic stress, labelled carbon was found exclusively in mannitol molecules (C_2 and C_5). Between 1 and 4h of stress, mannitol was degraded and 50% of labelled carbon originating from mannitol was allocated for glycerol synthesis and detected in $^{13}C_2$ glycerol. This result demonstrates that mannitol is not directly implicated in osmotic stress response but could contribute indirectly to osmoprotection via carbon relocation to glycerol molecules. This direct connection between mannitol and glycerol for stress answer underlines the central role of mannitol in *B. cinerea* carbon metabolism. In WT and single mutants, mannitol and trehalose disappearance correlated to glycerol accumulation (Figure 4). In order to participate to this transient response, trehalose could also be mobilized into glycerol.

Bcmpd deletion mutant reveals a mannitol phosphorylation pathway

Radial growth experiments revealed that *Bcmtdh* mutants were able to grow as well as the WT strain on mannitol, used as sole carbon source (Figure S4). Moreover, mannitol degradation occurred in *ΔBcmtdh* during osmotic stress response and during germination of spores. This degradation could be performed by the remaining MTDH activity detected in *ΔBcmtdh* or reveal that another pathway to degrade mannitol, via mannitol-1-phosphate probably, may exist. To confirm this hypothesis, WT, *ΔBcmpd* and *ΔBcmtdh* were grown for two days in the presence of 2% mannitol. Metabolic spectra of mycelial PCA extracts were then analyzed by *in vitro* ^{31}P-NMR spectroscopy. Mannitol-1-phosphate peaks were detected at 4.77 ppm for each strain. ^{31}P spectra of *ΔBcmpd* are presented in Figure 5. Mannitol-1-phosphate was detected after growth on mannitol, only. MPD is the only known enzyme in fungi able to produce mannitol-1-phosphate from fructose-6-phosphate [1]. Consequently, biosynthesis of mannitol-1-phosphate by *ΔBcmpd* requires a pathway which could phosphorylate mannitol into mannitol-1-phosphate. Moreover, *Bcmpd* and *Bcmtdh* gene expression analysis, performed after growth of WT strain on synthetic medium containing 2% mannitol as sole carbon source confirmed this hypothesis. In this case, *Bcmpd* expression level was 35 fold higher than *Bcmtdh* (Figure S5). This suggests that mannitol catabolism could occur through phosphorylation of mannitol and subsequent conversion in fructose-6-phosphate via MPD pathway.

Mannitol metabolism in fungi was proposed to occur as a cycle [12]. In this cycle, mannitol is synthesized through MPD pathway and degraded via MTDH pathway. However, several recent reports do not support the metabolism of mannitol operating as a cycle [4, 14]. The ability of the *ΔBcmpd* strains to use mannitol as sole carbon source clearly indicates that mannitol can be metabolized through other routes, most probably through mannitol-1-

phosphate. The remaining objection was the absence of mannitol kinase activity in fungi [2, 25]. In the present work, detection of mannitol-1-phosphate when *ΔBcmpd* mutants were grown on mannitol reveals for the first time the occurrence of a mannitol phosphorylation pathway in fungi. As a matter of fact, this phosphorylation of mannitol seems specific to fungi (at least to *B. cinerea*), since it has not been detected in any vascular plant cells or tissues that were preincubated in the presence of mannitol (Bligny, unpublished data). Accumulation of mannitol-1-phosphate could result from a one step reaction involving a mannitol kinase and ATP, or from a series of several enzymatic reactions that remain to be discovered.

Deletion of BcMPD and BcMTDH pathways did not abolish mannitol metabolism in *B. cinerea* and reveal a new metabolic route

Development and pathogenicity were not affected in Δ*Bcmpd* and Δ*Bcmtdh* mutant strains (Figure S2). *In vitro* and *in planta* conidiation and *in vitro* spore germination tests showed that mutant strains were not affected in those developmental steps. In that case, deletion of whole pathway by creating a *Bcmpd/Bcmtdh* double mutant was indispensable to assign a physiological role to mannitol.

To construct such a double deletion strain, *Bcmpd* mutant strain was transformed with a *Bcmtdh* disruption cassette containing a nourseothricin resistance marker (Figure S1A, B, C). To check deletion and homologous recombination, nourseothricin-resistant strains were screened by PCR (data not shown) and Southern blot (Figure S1D). Two strains, *db32.3* and *db35.2* were selected as double gene replacement mutants. Transcriptional analyses and western blotting confirmed deletion of both genes in the double mutants (Figure 2A, B). However, as found in the *ΔBcmtdh* single mutant, mannitol dehydrogenase activity was still detected in the double mutant strains, with a reduction of 70%, as compared to the wild type strain (Figure 2C).

Radial growth experiments revealed that the double mutants were able to grow as well as the WT strain on mannitol as sole carbon source (Figure S4). Furthermore, germination and sporulation and infection process were not altered in *ΔBcmpdΔBcmtdh* as compared to the WT strain (Figure S2). TLC profiles of intracellular sugars and polyols performed during development of *ΔBcmpdΔBcmtdh* revealed that mannitol was still produced in double mutants (Figure 6). While mannitol store was severely lowered in mycelium it was not affected in conidia (Figure 6). Quantification of intracellular metabolites by *in vitro* NMR spectroscopy in 2-day-old *ΔBcmpdΔBcmtdh* mycelium revealed that mannitol was synthetized from glucose and fructose (Table 2). As compared to the WT strain, mannitol content in *ΔBcmpdΔBcmtdh* mycelium after growth on glucose or fructose was decreased by 70% and 31%, respectively. The low mannitol dehydrogenase activity still detected in double mutant strains could explain why these mutants are still able to produce mannitol, principally from fructose. Moreover, this compound was still degraded during double mutant spore germination (Figure 6). This may suggest that the remaining mannitol dehydrogenase pathway could compensate mannitol production in double mutant conidia rather than in mycelium and be implicated in mannitol degradation during germination. Theses last findings strongly suggest that mannitol could be synthesized and degraded through potentially other metabolic routes.

Our data are in agreement with those reported in the case of *A. alternata* mtdh/mpd double mutant that was still able to grow on mannitol as sole carbon source [14]. In that case, the authors suggested that the fungus contain other enzymes that allow utilization of mannitol as a substrate. The ability of *B. cinerea* double mutant to metabolize mannitol, together with the presence of a mannitol dehydrogenase activity, suggest that additional unrelated mannitol

dehydrogenase encoding gene(s) should be present in *B. cinerea* genome. Recently, a new mannitol dehydrogenase showing no similarity with any known fungal MTDH has been described in *Tuber borchii* [35]. The phylogenetic analysis showed TbMDH to be the first example of a fungal mannitol dehydrogenase belonging to the medium-chain dehydrogenases/reductases (MDRs). Consequently, the *T. borchii* enzyme identified a new group of proteins forming a distinct subfamily of polyol dehydrogenase [35]. A BlastP search (http://www.broadinstitute.org/annotation/genome/botrytis_cinerea/Home.html) for possible homologies with *T. borchii Tbmdh* mannitol dehydrogenase [35] was thus performed. Surprisingly, our BlastP results clearly pointed out a *B. cinerea* sequence (BC1G_15343), annotated as an alcohol dehydrogenase, sharing 84% identity (89% positive) with TbMDH, while it shared only 11% identity with BcMTDH. In *T. borchii*, TbMDH produces mannitol from fructose. Such an enzyme, with a high preference for fructose and mannitol is a good candidate to perform mannitol synthesis from fructose and degrade mannitol during development in double mutant *B. cinerea* strains. However, further experiments are necessary to clearly implicate this new gene in *B. cinerea* mannitol metabolism.

In conclusion, a physiological role has been assigned to MTDH pathway that could be dedicated to a favourable conversion of fructose to mannitol and to mannitol degradation during osmotic stress response. On the other hand, we have shown that MPD pathway could also be implicated in mannitol catabolism, which abrogates the existence of a mannitol cycle. And finally, analyses of double mutant revealed the existence of a new mannitol pathway which could parallel mannitol dehydrogenase pathway functions. During plant infection, mannitol metabolism could help pathogen to efficiently sequestrate plant hexoses. Gene expression studies revealed a regulated developmental control for mannitol pathway. Interconnections of mannitol metabolism with the central carbohydrate pathway suggested that it could regulate carbon metabolic fluxes. Mannitol constitutes then an easily mobilisable carbon store, for growth and dissemination but also to cope with stresses and to maintain hyphal turgor pressure.

FUNDING

Thierry Dulermo was supported by a doctoral scholarship from the Région Rhône-Alpes (Cluster 9), France.

ACKNOWLEDGEMENTS

We thank Anne-Marie Boisson for technical assistance and M. Wésolowski-Louvel for critical reading of the manuscript.

REFERENCES

1 Lewis, D.H., and Smith, D.C. (1967) Sugar alcohols (polyols) in fungi and green plants. Distribution, physiology and metabolism. New Phytol. **66**, 143-184

2 Hult, K., Veide, A., and Gatenbeck, S. (1980) The distribution of the NADPH regenerating mannitol cycle among fungal species. Arch. Microbiol. **128**, 253-255

3 Feofilova, E.P., Tereshina, V.M., Garibova, L.V., Zav'ialova, L.A., Memorskaia, A.S., Maryshova, N.S. (2004) Germination of basidiospores of *Agaricus bisporus*. Prikl. Biokhim. Mikrobiol. **40**, 220-6

4 Solomon, P.S., Waters, O.D., Jörgens, C.I., Lowe, R.G., Rechberger, J., Trengove, R.D., and Oliver, R.P. (2006) Mannitol is required for asexual sporulation in the wheat pathogen *Stagonospora nodorum* (glume blotch). Biochem. J. **39**, 231-9

5 Ruijter, G.J., Bax, M., Patel, H., Flitter, S.J., van de Vondervoort, P.J., de Vries, R.P., vanKuyk, P.A., and Visser, J. (2003) Mannitol is required for stress tolerance in *Aspergillus niger* conidiospores. Eukaryot. Cell **2**, 690-8

6 Martin, F., Ramstedt, M., Söderhäll, K., and Canet, D. (1988) Carbohydrate and amino acid metabolism in the ectomycorrhizal ascomycete *Sphaerosporella brunnea* during glucose utilization. A ^{13}C NMR study. Plant Physiol. **86**, 935–940

7 Ceccaroli, P., Saltarelli, R., Cesari, P., Pierleoni, R., Sacconi, C., Vallorani, L., Rubini, P., Stocchi, V., and Martin, F. 2003. Carbohydrate and amino acid metabolism in *Tuber borchii* mycelium during glucose utilization: a (13)C NMR study. Fungal Genet. Biol. **39** , 168-75

8 Voegele, R.T., Hahn, M., Lohaus, G., Link, T., Heiser, I., and Mendgen, K. (2005) Possible roles for mannitol and mannitol dehydrogenase in the biotrophic plant pathogen *Uromyces fabae*. Plant Physiol. **137**, 190-8

9 Jennings, D.B., Ehrenshaft, M., Pharr, D.M., and Williamson, J.D. (1998) Roles for mannitol and mannitol dehydrogenase in active oxygen-mediated plant defense. Proc. Natl. Acad. Sci. U S A. **95,** 15129-15133

10 Vélëz, H., Glassbrook, N.J., and Daub, M.E. (2008). Mannitol biosynthesis is required for plant pathogenicity by *Alternaria alternata*. FEMS Microbiol. Lett. **285**, 122-129

11 Jennings, D.B., Daub, M.E., Pharr, D.M., and Williamson, J.D. (2002) Constitutive expression of a celery mannitol dehydrogenase in tobacco enhances resistance to the mannitol-secreting fungal pathogen *Alternaria alternata*. Plant J. **32**, 41-49

12 Hult, K., and Gatenbeck, S. (1978) Production of NADPH in the mannitol cycle and its relation to polyketide formation in *Alternaria alternata.* Eur. J. Biochem. **88**, 607-612

13 Solomon, P.S., Tan, K.C., and Oliver, R.P. (2005) Mannitol 1-phosphate metabolism is required for sporulation in planta of the wheat pathogen *Stagonospora nodorum*. Mol. Plant Mic. Int. **18,** 110-5

14 Vélëz, H., Glassbrook, N.J., and Daub, M.E. (2007) Mannitol metabolism in the phytopathogenic fungus *Alternaria alternata*. Fungal. Genet. Biol**. 4**, 258-68

15 Dulermo, T., Rascle, C., Chinnici, G., Gout, E., Bligny, R., and Cotton, P. (2009) Dynamic carbon transfer during pathogenesis of sunflower by the necrotrophic fungus *Botrytis cinerea*: from plant hexoses to mannitol. New Phytol. **183,** 1149-1162

16 Rolland, S., Jobic, C., Fèvre, M., and Bruel, C. (2003) *Agrobacterium*-mediated transformation of *Botrytis cinerea*, simple purification of monokaryotic transformants and rapid conidia-based identification of the transfer-DNA host genomic DNA flanking sequences. Curr. Genet. **44,** 164–171

17 Malonek, S., Rojas, M.C., Hedden, P., Gaskin, P. and Tudzynski, B. (2004) The NADPH: cytochrome P450 reductase gene from *Gibberella fujikuroi* is essential for gibberellin biosynthesis. J. Biol. Chem. **279,** 25075–25084

18 Hamada, W., Reignault, P., Bompeix, G., and Boccara, M. (1994) Transformation of *Botrytis cinerea* with the hygromycin B resistance gene, *hph*. Curr. Genet. **26**, 251-5

19 Church, G.M., Gilbert, W. (1984). Genomic sequencing. Proc Natl Acad Sci USA **81**, 1991-5

20 Verwoerd, B., Dekker, M.,and Hoekema, A. (1989) A small-scale procedure for the rapid isolation of plant RNAs. Nucleic Acids Res. **17,** 2362

21 Aubert, S., Gout, E., Bligny, R., Marty-Mazars, D., Barrieu, F., Alabouvette, J., Marty, F., and Douce, R. (1996) Ultrastructural and biochemical characterization of autophagy in higher plant cells subjected to carbon deprivation: control by the supply of mitochondria with respiratory substrates. J. Cell. Biol. **133**, 1251-1263

22 Suvarna, K., Bartiss, A., and Wong, B. (2000) Mannitol-1-phosphate dehydrogenase from *Cryptococcus neoformans* is a zinc-containing longchain alcohol/polyol dehydrogenase. Microbiology **146**, 2705-2713

23 Persson, B., Krook, M., andJornvall, H. (1991) Characteristics of short-chain alcohol dehydrogenases and related enzymes. *Eur J Biochem* **200,** 537-543

24 Jörnvall, H., Persson, B., Krook, M., Atrian, S., Gonzàlez-Duarte, R., Jeffery, J., and Ghosh, D. (1995) Short-chain dehydrogenases/reductases (SDR). Biochem. **34,** 6003-13

25 Solomon, P.S., Waters, O.D., and Oliver, R.P. (2007) Decoding the mannitol enigma in filamentous fungi. Trends Microbiol. **15,** 257-262

26 Doehlemann, G., Berndt, P., and Hahn, M. (2006) Trehalose metabolism is important for heat stress tolerance and spore germination of *Botrytis cinerea*. Microbiology **152**, 2625-2634

27 Jennings, D.H. (1984) Polyol metabolism in fungi. Adv. Microb. Physiol. **25**, 149-193

28 Jobic, C., Boisson, A.M., Gout, E., Rascle, C., Fèvre, M., Cotton, P., and Bligny, R. (2007) Metabolic processes and carbon nutrient exchanges between host and pathogen sustain the disease development during sunflower infection by *Sclerotinia sclerotiorum*. Planta **226,** 251-265

29 Olz, R., Larsson, K., Adler, L., and Gustafson, L. (1993) Energy flux and osmoregulation of *Saccharomyces cerevisiae* grown in chemostats under NaCl stress. J. Bacteriol. **175,** 2205–2213

30 d'Enfert, C., and Fontaine, T. (1997) Molecular characterization of the *Aspergillus nidulans treA* gene encoding an acid trehalase required for growth on trehalose. Mol. Microbiol. **24**, 203-216

31 Dixon, K.P., Xu, J.R., Smirnoff, N., and Talbot, N.J. (1999) Independent signaling pathways regulate cellular turgor during hyperosmotic stress and appressorium-mediated plant infection by *Magnaporthe grisea*. Plant Cell **11**, 2045-58

32 Clark, A.J., Blissett, K.J., and Oliver, R.P. (2003) Investigating the role of polyols in *Cladosporium fulvum* during growth under hyper-osmotic stress and *in planta*. Planta **216**, 614-9

33 Lowe, R.G., Lord, M., Rybak, K., Trengove, R.D., Oliver, R.P., and Solomon, P.S. (2008) A metabolomic approach to dissecting osmotic stress in the wheat pathogen *Stagonospora nodorum*. Fungal Genet. Biol**. 45,** 1479-86

34 Liu, W., Leroux, P., and Fillinger, S. (2008) The HOG1-like MAP kinase Sak1 of *Botrytis cinerea* is negatively regulated by the upstream histidine kinase Bos1 and is not involved in dicarboximide- and phenylpyrrole-resistance. Fungal Genet. Biol. **45,** 1062-1074

35 Ceccaroli, P., Saltarelli, R., Guescini, M., Polidori, E., Buffalini, M., Menotta, M., Pierleoni, R., Barbieri, E., and Stocchi, V. (2007) Identification and characterization of

the *Tuber borchii* D-mannitol dehydrogenase which defines a new subfamily within the polyol-specific medium chain dehydrogenases. Fungal Genet. Biol. **44**, 965-78

Tables :

Allocation of labelled carbon	Labelling transfer rate µmoles g^{-1} FW h^{-1}					
	3mM Glucose			3mM Fructose		
	WT	*ΔBcmpd*	*ΔBcmtdh*	WT	*ΔBcmpd*	*ΔBcmtdh*
Glycogen	0.9	1.4	0.3	n.d.	n.d.	n.d.
Mannitol C1/6	0.55	0.09	0.5	n.d.	n.d.	n.d.
Mannitol C2/5	n.d.	n.d.	n.d.	1.4	1.37	1
Trehalose C6	0.39	0.73	0.08	n.d.	n.d.	n.d.

Table 1 Transfer rates of labelled hexoses through carbon mannitol metabolism in *B. cinerea* WT strain and single mutants.
Transfer rates were obtained from proton-decoupled ^{13}C-NMR *in vivo* spectra of sunflower cotyledons infected by *B. cinerea* (48 hpi). At time zero, 3 mM [1-^{13}C]glucose or 3 mM [2-^{13}C]fructose were added to perfusion medium. Sugar conversion was analysed during 3.5 h. Transfer rates were determined at the end of the analysis period. Spectral conditions were as given in experimental procedures. Two independent experiments were done from separate infection series and cultures. A representative result is presented. n.d., not detected.

	2% Glucose				2% Fructose			
	WT	*ΔBcmpd*	*ΔBcmtdh*	*ΔBcmtdh ΔBcmpd*	WT	*ΔBcmpd*	*ΔBcmtdh*	*ΔBcmtdh ΔBcmpd*
Glucose	0.8	0.7	0.9	1.0	n.d.	n.d.	n.d.	n.d.
Fructose	n.d.	n.d.	n.d.	n.d.	1.0	0.8	1.4	0.4
Mannitol	10.9	1.3	4.9	2.8	18.2	10.2	5.8	11.0
Tréhalose	1.0	6.6	n.d.	6.4	0.3	n.d.	n.d.	n.d.
Arabitol	0.3	0.6	0.7	0.5	1.0	1.5	1.3	1.3
Glycérol	7.7	6.7	3.7	5.9	4.1	1.2	0.5	0.8

Table 2 Impact of carbon sources on polyol and sugar content of WT, *ΔBcmpd, ΔBcmtdh, ΔBcmpdΔBcmtdh*

ΔBcmpdΔBcmtdh strains were grown 2-d on 2% glucose or 2% fructose. Sugars and polyols were extracted and analysed by NMR in vitro spectroscopy, as described in experimental procedures. Two independent experiments were done from separate cultures. A representative result is presented. n.d., not detected

Figure Legends

Figure 1 Model showing mannitol metabolism and main carbohydrate conversion pathways in fungi

Dotted arrows indicate series of enzymatic reactions.

Figure 2 Effect of mannitol pathway alteration on *Bcmpd* and *Bcmtdh* transcript levels, proteins and enzymatic activities

Mycelia were cultivated 2-d, on synthetic medium supplemented with 2% glucose. (**A**) *Bcmpd* and *Bcmtdh* gene expression. *Bcmpd* and *Bcmtdh* gene expression was measured by quantitative PCR using gene-specific primers and calibrated to *BcactA* transcripts. Amplifications were done in triplicate, from 3 independent biological replicates. Bars represent SD. (**B**) BcMPD and BcMTDH detection by western blot analysis. Gels were loaded with 75 µg of proteins in each lane. Western blots were repeated twice, representative results are presented here. (**C**) BcMPD and BcMTDH enzymatic activities. Total mannitol-1-phosphate dehydrogenase and mannitol dehydrogenase activities were measured from 50 µg of proteins by monitoring absorbances changes of $NAD(P)^{+}/NAD(P)H$ at 340 nm. Analyses were performed in duplicate from two independent biological replicates. A representative result is presented here.

Figure 3 Sugars content and *Bcmpd* and *Bcmtdh* transcript levels during *in vitro* development

(**A**) Sugars and polyols were extracted from 12-d-old fresh spores (conidia), germinating conidia (2, 4, and 6 h after activation of spore germination in rich liquid medium), young mycelium (2-d-old) and sporulating mycelium (6-d-old), after growth of WT strain, *ΔBcmpd* and *ΔBcmtdh* in the presence of glucose. Fungal extracts were then analysed by TLC as described in experimental procedures. Sugars and polyols were extracted from at least three independent biological replicates. A representative chromatography is presented here. (**B**) Total RNA was extracted from WT strain. *Bcmpd* and *Bcmtdh* gene expression was measured by quantitative PCR using gene-specific primers and calibrated to *BcactA* transcripts. RNA was extracted from at least three independent biological replicates. Bars represent SD. (**C**) Detection of BcMPD and BcMTDH in WT conidia and germinating conidia by Western blot analysis. Gels were loaded with 75 µg of proteins in each lane. Proteins were extracted from at least three independent biological replicates. A representative western blot is presented here.

Figure 4 Intracellular sugar content and *Bcmpd* and *Bcmtdh* transcript levels in WT, *ΔBcmpd,* and *ΔBcmtdh* during an osmotic stress response

Sugar, polyols and total RNA were extracted from young mycelium cultivated for 2 d on synthetic medium supplemented with 2% glucose and then transferred 0, 0.5, 1, 4, 6, 9 or 24 h on the same medium supplemented with 1M NaCl. (**A**) Analysis of mannitol, trehalose and glycerol content in WT and mannitol mutant strains was performed by TLC experiments. Culture transfers and TLC experiments were repeated three times from independent biological replicates. Representative chromatographies are presented here. (**B**) *Bcmpd* and *Bcmtdh* gene expression was quantified, in WT and mutant strains, by PCR using gene-specific primers and

was calibrated to *BcactA* transcripts. Amplifications were done in triplicate from 3 independent biological replicates. Bars represent SD. (**C**) Western blot detection of BcMPD and BcMTDH in WT, *ΔBcmpd* and *ΔBcmtdh* strains. Gels were loaded with 75 µg of proteins in each lane. Proteins were extracted from at least three independent biological replicates. Representative results are presented here.

Figure 5 ***Bcmpd*** **deletion mutant reveals a mannitol phosphorylation pathway in** ***B. cinerea***

Proton-decoupled ^{31}P-NMR spectra of PCA extracts of *ΔBcmpd* mycelium during growth in the presence of mannitol as sole carbon source**.** Extracts were prepared from 5 to 10 g of mycelium grown on 2% glucose (**A**) or on 2% mannitol (**B**). Peaks assignments are as follows: Mnt-1-P, mannitol-1-phosphate; Glcn-6-P, 6-phosphogluconate; α/β-Glc-6-P, α/β-glucose-6-phosphate; Tre-6-P, trehalose-6-phosphate; Gly-3-P, glycerol-3-phosphate; PGA, Phosphoglyceric acid; n.d., not determined. This experiment was done twice. Representative spectra are presented here.

Figure 6 **Sugar and polyol content during** ***in vitro*** **development of** ***ΔBcmpdΔBcmtdh***

Sugars and polyols were extracted from 2-day-old double mutant mycelium after growth in the presence of 2% glucose and analysed by TLC as described in experimental procedures. This experiment was done in triplicate using independent biological replicates. A representative chromatograph is presented here.

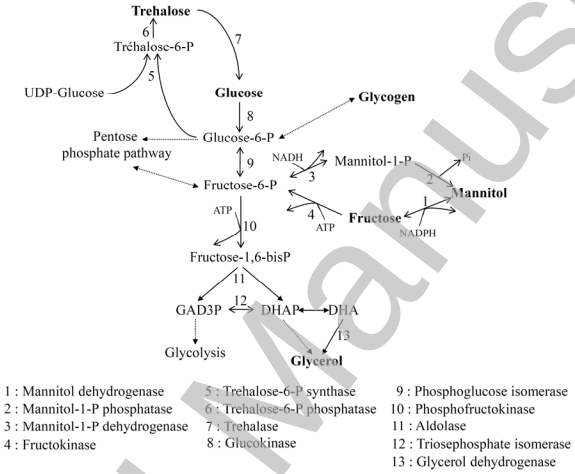

Figure1.tif

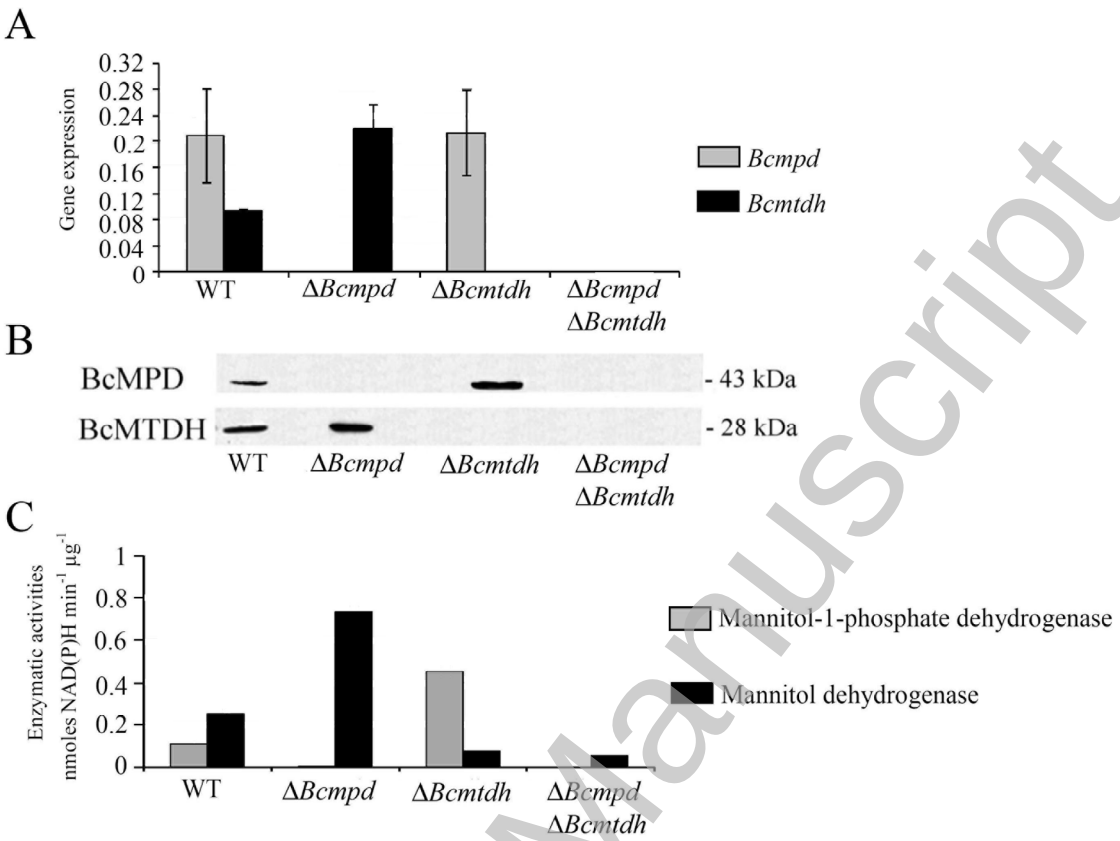

Figure2.tif

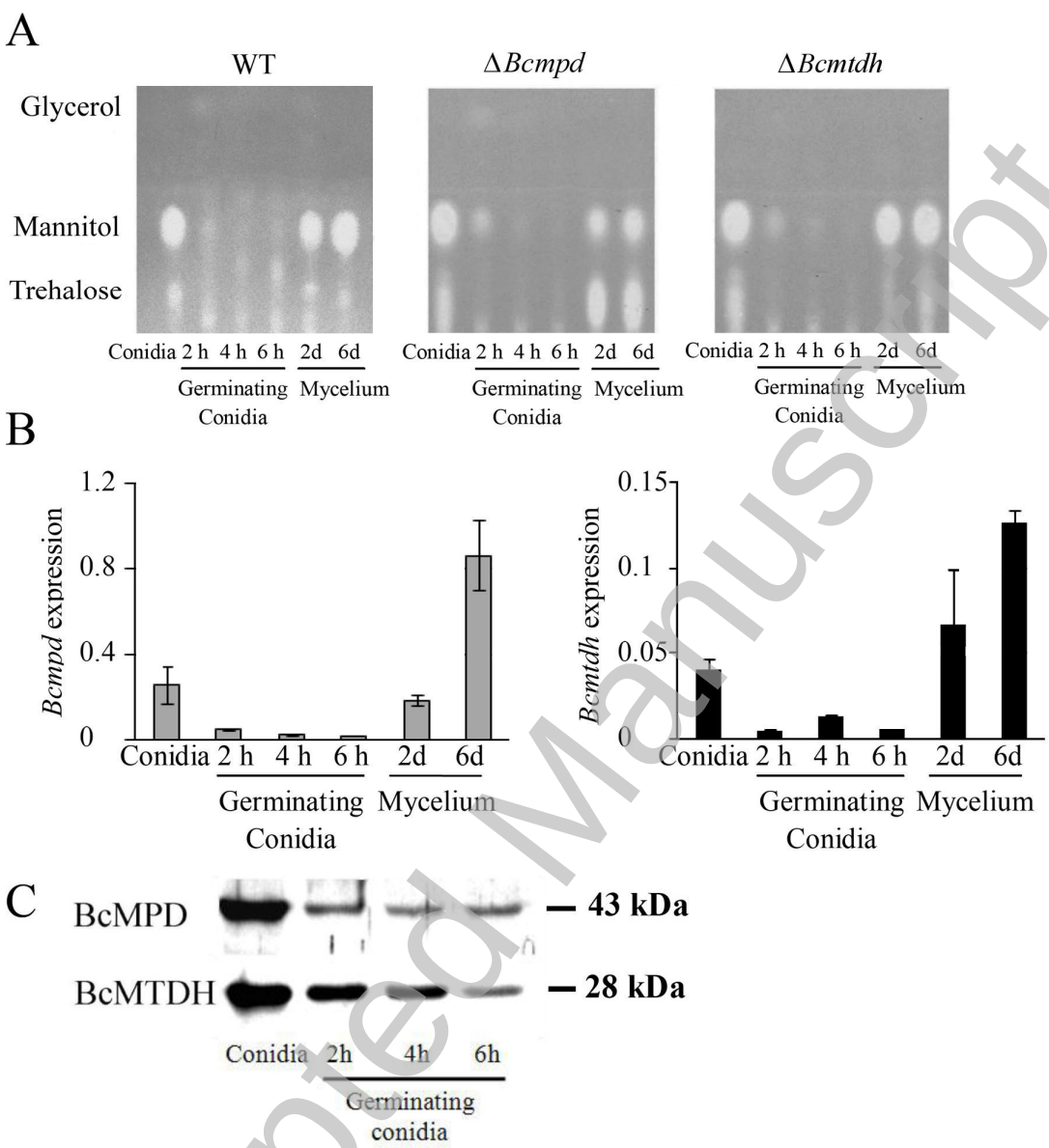

Figure3.tif

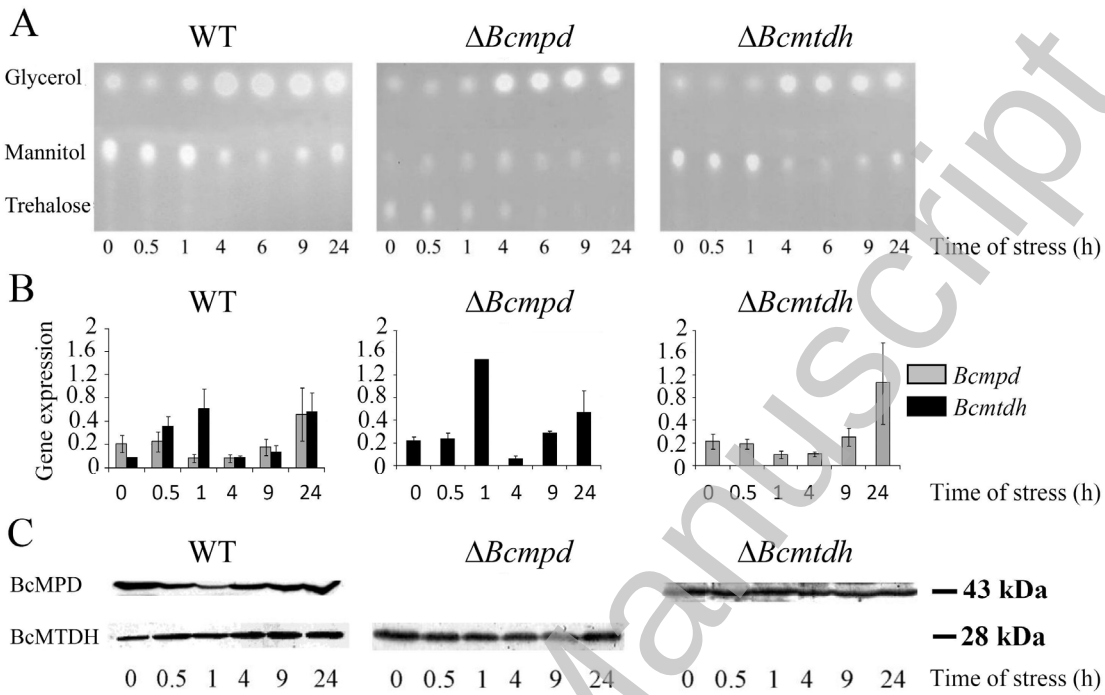

Figure4.tif

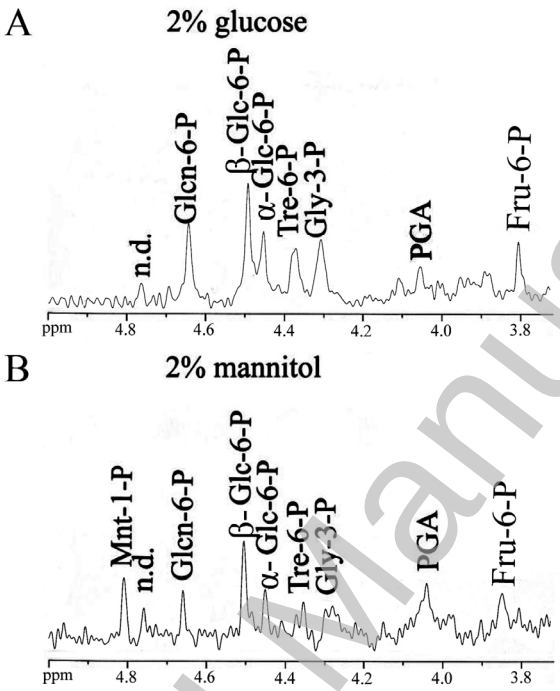

Figure5.tif

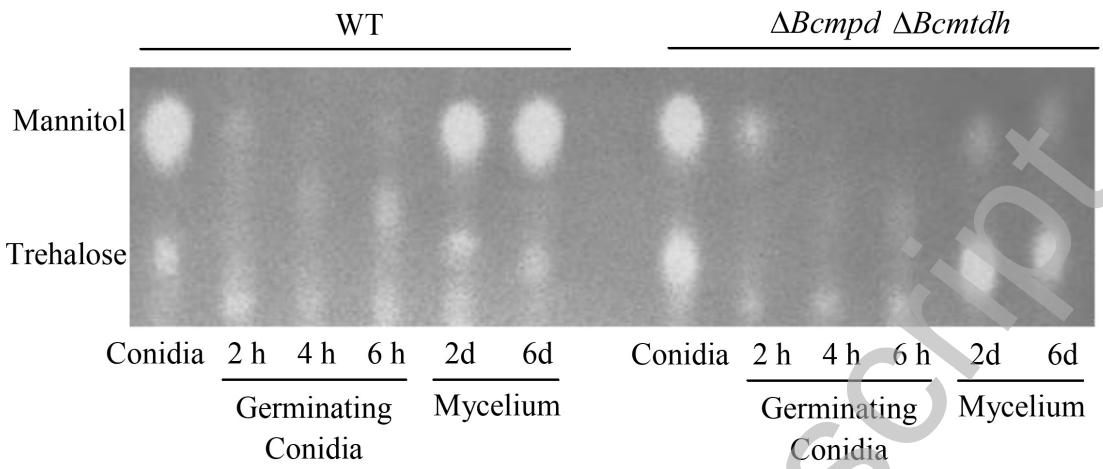

Figure6.tif